Human Molecular Genetics, 2013, Vol. 22, No. 17 **3568–3582**
doi:10.1093/hmg/ddt211
Advance Access published on May 12, 2013

Bcl6a function is required during optic cup formation to prevent p53-dependent apoptosis and colobomata

Jiwoon Lee[1], Bum-Kyu Lee[1] and Jeffrey M. Gross[1,2,*]

[1]Section of Molecular Cell and Developmental Biology, Institute for Cellular and Molecular Biology and [2]Institute of Neuroscience, University of Texas at Austin, Austin, TX 78712, USA

Received March 25, 2013; Revised March 25, 2013; Accepted May 1, 2013

Mutations in *BCOR* (Bcl6 corepressor) are found in patients with oculo-facio-cardio-dental (OFCD) syndrome, a congenital disorder affecting visual system development, and loss-of-function studies in zebrafish and *Xenopus* demonstrate a role for Bcor during normal optic cup development in preventing colobomata. The mechanism whereby BCOR functions during eye development to prevent colobomata is not known, but in other contexts it serves as a transcriptional corepressor that potentiates transcriptional repression by B cell leukemia/lymphoma 6 (BCL6). Here, we have explored the function of the zebrafish ortholog of Bcl6, Bcl6a, during eye development, and our results demonstrate that Bcl6a, like Bcor, is required to prevent colobomata during optic cup formation. Our data demonstrate that Bcl6a acts downstream of Vax1 and Vax2, known regulators of ventral optic cup formation and choroid fissure closure, and that *bcl6a* is a direct target of Vax2. Together, this regulatory network functions to repress *p53* expression and thereby suppress apoptosis in the developing optic cup. Furthermore, our data demonstrate that Bcl6a functions cooperatively with Bcor, Rnf2 and Hdac1 in a common gene regulatory network that acts to repress *p53* and prevent colobomata. Together, these data support a model in which p53-dependent apoptosis needs to be tightly regulated for normal optic cup formation and that Bcl6a, Bcor, Rnf2 and Hdac1 activities mediate this regulation.

INTRODUCTION

Colobomata are developmental defects of the eye which result in a cleft or absence of tissue in one or more ocular structures (1–3). Colobomata are also a common phenotypic manifestation in over 50 distinct human genetic disorders (OMIM: http://www.ncbi.nlm.nih.gov/), and they are estimated to be present in 3–10% of all blind children worldwide (4,5). During normal ocular morphogenesis, a region of the ventral optic cup called the choroid fissure must close in order to prevent colobomata. While choroid fissure closure is a critical aspect of ocular development that requires a precise interplay between growth, morphogenesis and regulated gene expression, the molecular and cellular mechanisms underlying this process have not yet been fully elucidated in any vertebrate organism (1).

Mutations in *BCOR* (Bcl6 Corepressor) have been found in patients with oculo-facio-cardio-dental (OFCD; OMIM 300166) syndrome, an X-linked condition in which afflicted patients display ocular abnormalities, cardiac septation defects and dental anomalies (6–9). Ocular defects in OFCD patients include microphthalmia, cataracts and higher risk of glaucoma (8). The mechanism whereby BCOR functions during eye development is not known, but in other contexts it serves as a transcriptional corepressor that potentiates transcriptional repression by B cell leukemia/lymphoma 6 (BCL6) (10). Knockdown of BCOR in zebrafish and *Xenopus* embryos results in OFCD-like ocular defects including microphthalmia and colobomata, as well as skeletal and central nervous system (CNS) abnormalities (8,11). BCOR is a core part of a transcriptional repression complex containing Ring finger protein 2 (RNF2), an E3 ubiquitin ligase that ubiquitinates histone H2A, and FBXL10/JHDM1B, an F-box protein with a JmjC domain that functions in H3K36 demethylation (12). H2A ubiquitination and H3K36 demethylation both lead to transcriptional repression (13,14), suggesting that BCOR function may be required to mediate epigenetic silencing during development (15).

The BCOR complex is recruited to target genes by BCL6, and target genes include *p53* and *cyclin D2* in B cells (15). *BCL6* encodes a sequence-specific transcriptional repressor (16,17) that has been extensively studied for its role as a proto-oncogene and its involvement in certain types of lymphomas (18–20). BCL6 is required for germinal-center formation in mouse (21),

*To whom correspondence should be addressed. Tel: +1 512 4711518; Fax: +1 512 4713878; Email: jmgross@austin.utexas.edu

where it functions to repress *p53* expression in order to prevent apoptosis that would be otherwise triggered by DNA breaks occurring during immunoglobulin class switch recombination (22). While the involvement of BCL6 in B cell development and lymphomagenesis has been well studied in knockout mice (21,22) and cell culture (23), its functions during embryonic development remain poorly elucidated. Outside of the immune system, BCL6 is known to function in the development of the olfactory system, where it also serves as an anti-apoptotic factor during olfactory sensory neuron differentiation (24). Recently, BCL6 has been reported to be involved in the development of left-right asymmetry during *Xenopus* embryogenesis by inhibiting Notch target genes and thereby maintaining the expression of *Pitx2* in the left lateral plate mesoderm (25). Interestingly, BCOR is also involved in the development of left–right asymmetry, suggesting a conserved developmental role for BCL6-mediated BCOR repression in this process (11).

In addition to BCOR, BCL6 is also known to require association with regulatory complexes containing histone deacetylases (HDACs), and other transcriptional co-repressors, in order to repress transcription of target genes (26–28). In zebrafish, a *hdac1* mutation results in colobomata (29,30). Moreover, in retinal cell culture, pharmacological inhibition of Hdac function by trichostatin A (TSA) results in elevated expression of the pro-apoptotic protein, Apaf-1, via upregulation of *p53*, suggesting that Hdac activity may be required to prevent apoptosis in the retina (31,32).

Our interest is in determining the molecular and cellular mechanisms contributing to optic cup formation and choroid fissure closure. Our studies utilize the zebrafish, *Danio rerio*, as a model system for studying these processes. Many disrupted genes and pathways identified as integral to the formation of the zebrafish eye produce phenotypes that resemble disorders of the human visual system (33–35). Indeed, zebrafish have been a useful model for studying colobomata; loss-of-function phenotypes for *aussicht*, *pax2a*, *vax1* and *vax2*, *fgf19*, *n-cadherin*, *apc*, *laminin β1*, *laminin γ1*, *patched2*, *bcor*, *hdac1*, *nlz1* and *nlz2* and *tfap2* (8,29,30,36–48) each lead to colobomata in zebrafish, and these have been informative in furthering our understanding of choroid fissure closure *in vivo*. Of particular interest among this group of genes are *vax1* and *vax2*. Vax1 and Vax2 are co-expressed in the optic stalk and ventral retina, and their expression overlaps with *bcl6a* (40,49–51). Knockout of either *Vax1* or *Vax2* leads to ventral optic cup defects and colobomata in mouse (52–55), and similarly, morpholino disruption of both *vax1* and *vax2* in zebrafish results in ventral optic cup defects and colobomata (40). Recently, Viringipurampeer *et al*. demonstrated that Vax2, along with Pax2, regulate the expression of the *fas-associated death domain* gene (*fadd*) in zebrafish (56). Deletions of *FADD* segregate with colobomata in human patients (57), and these have been modeled through morpholino knockdown in zebrafish (56). *fadd*-deficient embryos possess elevated levels of necroptotic cell death throughout the retina, and these correlate with colobomata (56), suggesting that Fadd-mediated suppression of necroptotic cell death may be a critical component of normal optic cup development in order to prevent colobomata.

Given that mutations in *BCOR* were found in OFCD patients (8), and knockdown of zebrafish and *Xenopus* orthologs of *bcor* resulted in ocular abnormalities that included colobomata, we were curious whether Bcl6 itself is required for normal eye development and, if so, whether it acts in conjunction with Bcor or other co-repressors in mediating these effects. Here, we demonstrate that loss of Bcl6a function leads to colobomata in zebrafish. Our data support a model in which Bcl6a expression is regulated by Vax1 and Vax2, and that Bcl6a functions in a genetic pathway that includes Bcor, Rnf2 and Hdac. These factors function to repress *p53* expression, thereby preventing apoptotic cell death and colobomata during optic cup development.

RESULTS

bcl6a is expressed in the ventral optic cup and choroid fissure

bcl6a expression in zebrafish has been reported from a high-throughput expression screen (58), and here, we both confirmed these patterns and provided a more detailed spatiotemporal analysis of expression during eye development. *bcl6a* is expressed in the lens and myotome prior to 24 hpf (58; data not shown). In the retina, *bcl6a* begins to be expressed near the choroid fissure at 30 hpf, and this domain expands into the ventronasal retina at 39 hpf (Fig. 1A–C). Transcripts expand both nasally and temporally in the outermost region of the ventral retina by 48 hpf, and *bcl6a* is detected in most of the ventral retina by 54 hpf (Fig. 1D–F). *bcl6a* is also expressed in the forebrain at 39 hpf (Fig. 1C) and the optic tectum from 39 to 54 hpf (Fig. 1G and H).

Knockdown of Bcl6a results in colobomata

To determine whether Bcl6a is required for normal ocular development, we utilized morpholino knockdown in zebrafish (59,60). Morpholinos were designed to the translation start site of *bcl6a* (*bcl6a*-ATGMO) and the exon2/intron2 splice junction (*bcl6a*-SPMO). Injection of either morpholino resulted in colobomata (Fig. 2 and Supplementary Material, Fig. S1); data are presented for *bcl6a*-SPMO since we could readily verify its efficiency in disrupting *bcl6a* splicing in each subsequent experiment (Fig. 2O). Injection of 7.5 ng of *bcl6a*-SPMO resulted in embryos with laterally curved bodies and colobomata at 3 dpf (Fig. 2B, E–H), while 5 bp mismatch morpholino (*bcl6a*-MM) injected embryos developed normally (Fig. 2A, C and D). By 5 dpf, colobomata in *bcl6a*-SPMO injected embryos were more severe, with Bcl6a-deficient embryos possessing obvious holes in the posterior of the eye through which retinal and RPE tissue were extruded into the forebrain (Fig. 2K–N). Histological analyses of the *bcl6a*-SPMO and *bcl6a*-MM injected embryos highlight the colobomata in Bcl6a-deficient embryos. While retinal lamination, lens and RPE formation appeared to be largely unaffected (Fig. 2J), and all retinal cell types were present in the Bcl6-deficient embryos (data not shown), colobomata were obvious wherein a large region of the choroid fissure remained open (Fig. 2I and J).

Previous studies in *Xenopus* have demonstrated that BCL6 is required for left-right patterning during development (25); in this study, morpholino knockdown resulted in defects in heart positioning and gut rotation. To determine if Bcl6a functions similarly in zebrafish, *cmlc2* expression was examined, which serves as a marker of left/right position of the developing heart. 100% of

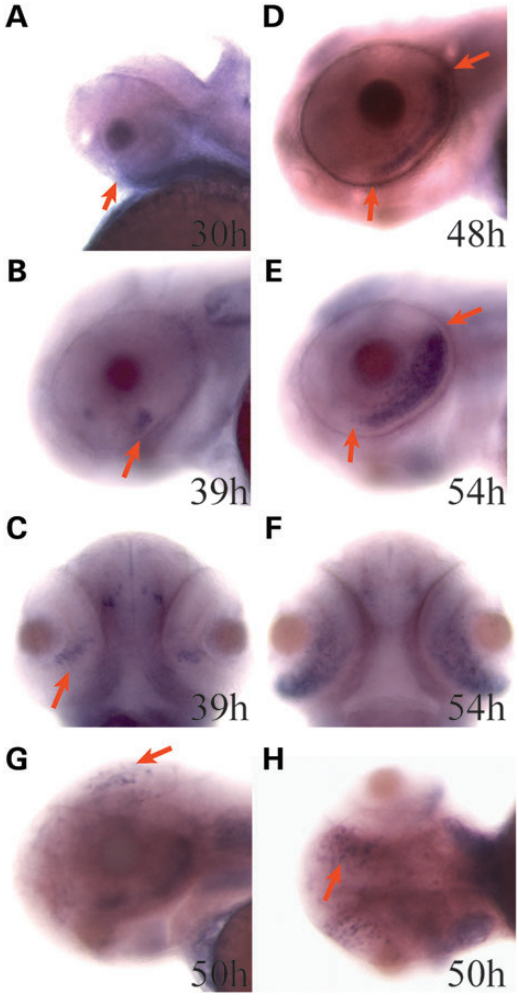

Figure 1. Expression pattern of *bcl6a* in the zebrafish eye. *bcl6a* expression in the retina of wild-type embryos at (**A**) 30 hpf, (**B** and **C**) 39 hpf, (**D**) 48 hpf, and (**E** and **F**) 54 hpf imaged (A, B, D and E) laterally and (C and F) ventrally. (A) *bcl6a* expression is observed in the choroid fissure at 30 hpf (arrow), and (B–F) later expands into the ventral retina (arrows B–E). *bcl6a* expression in the optic tectum at 50 hpf (arrow) imaged (**G**) laterally and (**H**) dorsally. Dorsal is up in A, B, D, E and G. Anterior is up in (F), left in (H).

bcl6a-MM injected embryos possessed a left-sided orientation of the heart ($n = 41$ embryos), whereas *bcl6a*-SPMO injected embryos possessed a randomized orientation of heart, with embryos presenting with left-sided (53.7%), right-sided (31.9%) or no orientation (14.4%) ($n = 41$ embryos; $P < 0.01$) (Supplementary Material, Fig. S2).

Morpholino injection can cause off-target effects in a sequence-specific manner (61). To determine whether colobomata in *bcl6a*-SPMO and *bcl6a*-ATGMO injected embryos were specific to the knockdown of Bcl6a, *bcl6a*-SPMO and *bcl6a*-ATGMO were co-injected at sub-threshold levels (i.e. those that do not lead to a colobomata when injected alone) and phenotypes assessed. When the injection amount of *bcl6a*-SPMO was reduced from 7.5 to 2.5 ng, no embryos showed colobomata. Similarly, when *bcl6a*-ATGMO was injected at 2.5 ng/embryo, development was normal (Supplementary Material, Fig. S3). However, co-injection of 2.5 ng *bcl6a*-SPMO and 2.5 ng *bcl6a*-ATGMO resulted in colobomata in all embryos ($n = 23$) (Supplementary Material, Fig. S3). Furthermore, co-injection of 250 pg *bcl6a* mRNA with 7.5 ng *bcl6a*-SPMO was highly effective in reducing the incidence of colobomata in *bcl6a*-SPMO injected embryos (Fig. 3A–D). In *bcl6a*-SPMO injected embryos, 65.2% possessed colobomata, and co-injection of *bcl6a* mRNA suppressed this to 11.3% ($P < 0.01$) (Fig. 3D). Taken together, these data support the notion that colobomata in *bcl6a* morpholino-injected embryos are a specific result of Bcl6a deficiency and not due to morpholino toxicity.

Previous studies have reported that Bcor deficiency in zebrafish and *Xenopus laevis* embryos resulted in colobomata, indicating a conserved function for Bcor among these vertebrates (8,11). Thus, we investigated whether Bcl6 function was also required during *Xenopus laevis* eye formation. Injection of a translation blocking morpholino (*xbcl6*-MO) targeting *Xenopus bcl6* into one dorsal blastomere at the four-cell stage, whose cells are fated to give rise to CNS and eye field (62), resulted in colobomata in 76% of injected embryos ($n = 25$) when compared with control-injected embryos, and the contralateral uninjected side (Fig. 3E–H). Combined, these results strongly support a model in which Bcl6 function is required for normal eye development in both zebrafish and *Xenopus* embryos; loss of Bcl6 function in either system results in colobomata.

Bcl6a prevents cell death in the retina by suppressing *p53* expression

BCL6 is required to prevent p53-dependent apoptosis that results from hypermutation and chromosome rearrangement in germinal center B cells (22). Thus, we reasoned that Bcl6a may play a similar role in the eye, and that elevated apoptosis may be the cellular mechanism leading to colobomata in Bcl6a-deficient embryos. To begin testing this hypothesis, TUNEL analyses were performed to detect apoptotic cells in *bcl6a*-MM and *bcl6a*-SPMO injected embryos at 48 hpf, a time at which there are typically no apoptotic cells in the retina of wild-type embryos (63). Indeed, *bcl6a*-MM injected embryos possessed no apoptotic cells (100%, $n = 17$), while there were numerous apoptotic cells in most *bcl6a*-SPMO injected embryos (76%, $n = 21$) (Fig. 4A and B). We next quantitatively assessed whether Bcl6a regulates *p53* expression in zebrafish. Quantification of *p53* expression at 48 hpf by qRT–PCR revealed that *p53* levels were 2.3 times higher in *bcl6a*-SPMO injected embryos than in *bcl6a*-MM injected embryos ($P < 0.0001$) (Fig. 4C). To determine whether increased *p53* levels were responsible for colobomata in *bcl6a*-SPMO injected embryos, we attempted to rescue the phenotype by reducing p53 levels through morpholino knockdown. Co-injection of 7.5 ng *bcl6a*-SPMO and 7.5 ng *bcl6a*-MM (as a 'load' control) resulted in colobomata, as in previous experiments (Fig. 4F and G). However, all embryos co-injected with 7.5 ng *bcl6a*-SPMO and 7.5 ng *p53* morpholino (*p53*-MO) developed normally ($n = 25$; Fig. 4H and I), indicating that reduction of p53 rescued colobomata. These data support a model in which Bcl6a functions as a regulator of apoptosis by controlling *p53* expression in the developing optic cup, and that Bcl6a-dependent repression of *p53* is required to prevent apoptosis during normal eye development.

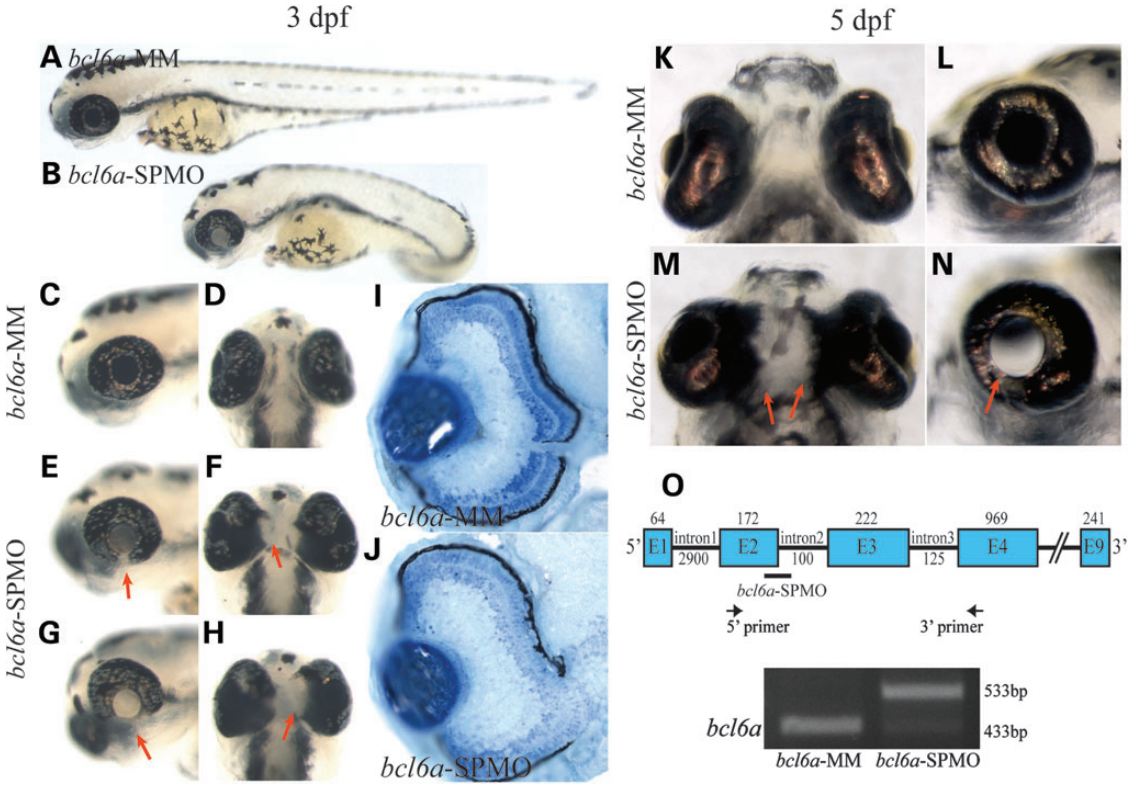

Figure 2. Knockdown of Bcl6a causes colobomata in zebrafish. (**A**, **C** and **D**) *bcl6a*-MM and (**B**, **E**–**H**) *bcl6a*-SPMO injected embryos at 3 dpf imaged (A–C, E and G) laterally and (**D**, F and H) ventrally. Transverse histological sectioning of (**I**) *bcl6a*-MM and (**J**) *bcl6a*-SPMO injected embryos. 7.5 ng injection of *bcl6a*-SPMO targeting *bcl6a* transcript resulted in curved bodies and colobomata. (**K** and **L**) *bcl6a*-MM and (**M** and **N**) *bcl6a*-SPMO injected embryos at 5 dpf imaged (K and M) ventrally, and (L and N) laterally. By 5 dpf, (M and N) colobomata in *bcl6a*-SPMO injected embryos are more severe, with (M) Bcl6a-deficient embryos displaying extruded retina and RPE tissue into the forebrain and (N) an obvious non-pigmented 'hole' in the eye, when imaged through the lens. (**O**) Efficiency of *bcl6a*-SPMO in disrupting *bcl6a* splicing validated by RT–PCR in *bcl6a*-MM injected and *bcl6a*-SPMO injected embryos. Injection of *bcl6a*-SPMO resulted in the inclusion of intron2 (100 bp) into *bcl6a* transcripts, creating a frameshift and premature stop codon when translated. Dorsal is up in A–C, E, G, I, J, L and N. Anterior is up in D, F, H, K and M.

Overproliferation within the retinal neuroepithelium has been shown to be a cause of colobomata in mice (64), and reduced proliferation has been hypothesized to also lead to colobomata (1). Thus, we wanted to determine whether retinoblast proliferation was affected in Bcl6a-deficient embryos. To quantify retinoblast proliferation, we stained embryos for phosphohistone H3 (pH3), a marker of late G2/M phase and quantified the number of $pH3^{+}$ cells/retinal area. No differences in proliferation were identified between *bcl6a*-SPMO and *bcl6a*-MM injected embryos at 52 hpf (Supplementary Material, Fig. S4), indicating that changes in retinoblast proliferation are not likely to underlie colobomata in Bcl6a-deficient embryos.

Vax1 and Vax2 regulate the expression of *bcl6a* in the ventral retina

vax1 and *vax2* are expressed in the optic stalk and the ventral optic cup, and their expression domains overlap spatially and temporally with that of *bcl6a* (40). A loss of Vax1 and Vax2 function results in colobomata in mouse, combined morpholino knockdown in zebrafish also results in colobomata (40,52–55) and Vax2 has been recently shown to regulate *fadd* expression to prevent cell death and colobomata in zebrafish (56). Thus, we hypothesized that Vax1 and Vax2 may function as upstream regulators of *bcl6a* during eye development. To begin testing this hypothesis, *in situ* hybridization was utilized to determine whether *bcl6a* expression required Vax1 and Vax2 activity. While *bcl6a* was expressed in the ventral retina of control morpholino (conMO) injected embryos at 48 hpf, *bcl6a* was not detected in the retina of *vax1* and *2*-MO injected embryos (Fig. 5A and B). To determine whether Vax2 directly regulates *bcl6a* expression, chromatin immunoprecipitation (ChIP) analyses were performed. A consensus zebrafish Vax2 binding sequence (TCATTA) was identified bioinformatically 214 bp upstream of the translation start site of *bcl6a*, and this region was utilized in qRT–PCR assays to quantify enrichment in ChIP samples. While a Vax2 antiserum that recognizes zebrafish protein has been reported in the literature (56), we were unable to validate a specific interaction when using this serum. Thus, we utilized an alternative approach, that is by generating a *myc*-tagged version of *vax2* and injecting this into zebrafish embryos, we then performed ChIP using an anti-Myc antibody, an approach that has been successfully utilized in numerous other ChIP assays when cross-reactive antibodies are unavailable (65–67). Expression of *myc-vax2* and anti-Myc ChIP resulted in a 2.23-fold enrichment by qRT–PCR of the Vax2 binding site containing region when compared with a ChIP sample isolated using a negative control antibody (Fig. 5C;

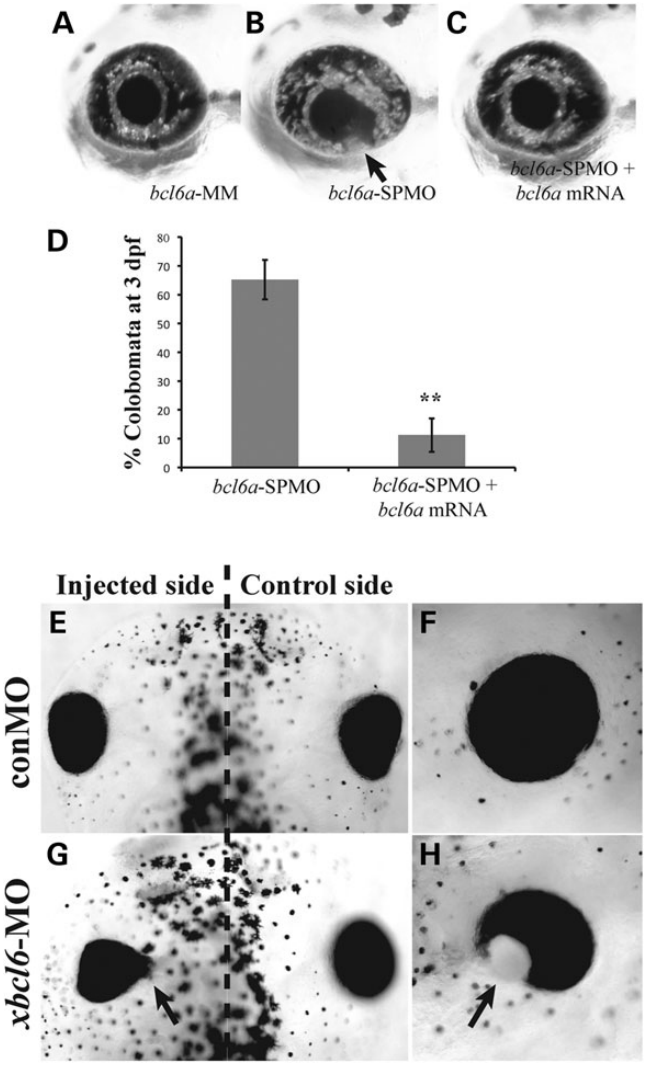

Figure 3. Loss of Bcl6a function is responsible for colobomata in zebrafish and *Xenopus*. (**A**–**D**) Injection of *bcl6a* mRNA significantly reduced the incidence of coloboma in Bcl6a-deficient embryos. In (B), *bcl6a*-SPMO injected embryos, 65.2% displayed coloboma ($n = 40/61$), and (C) co-injection of *bcl6a* mRNA suppressed this to 11.3% ($n = 9/89$) ($P < 0.01$). (**E** and **F**) conMO and (**G** and **H**) translation blocking morpholino targeting *Xenopus bcl6* transcripts (*xbcl6*-MO) injected *Xenopus* embryos were imaged at stage 41 (E and G) dorsally and (F and H) laterally. (G) Injection of 40 ng *xbcl6*-MO results in coloboma, and (H) a medial displacement of ventral retina tissue (arrow). Injected side is left in (E) and (G). Anterior is up in (E) and (G). Dorsal is up in (A–C, F, H).

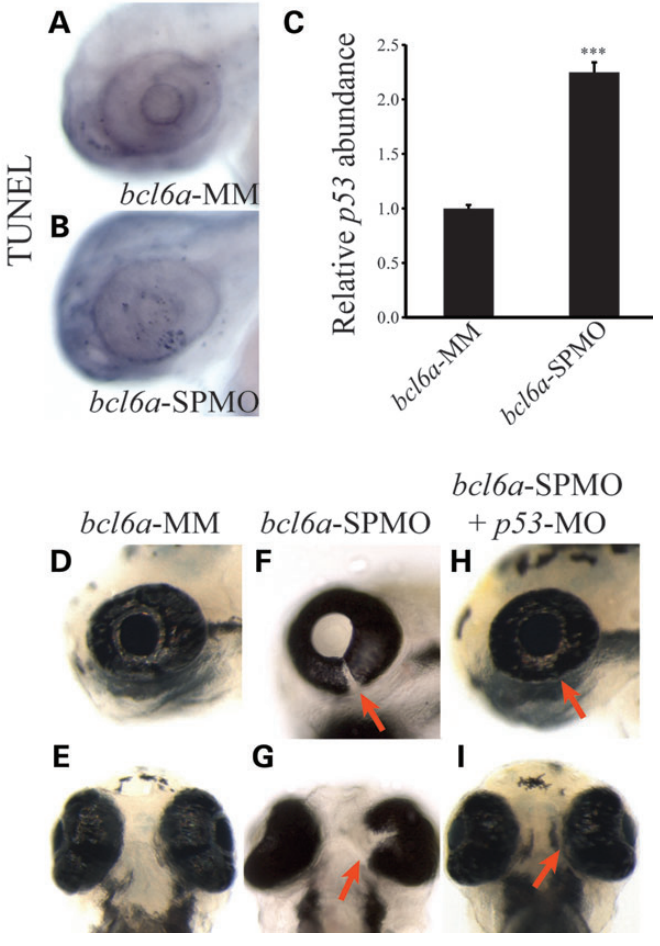

Figure 4. Loss of Bcl6a function results in increased apoptosis and *p53* expression, and this is responsible for colobomata. TUNEL analysis in (**A**) *bcl6a*-MM and (**B**) *bcl6a*-SPMO injected embryos at 48 hpf. Bcl6a-deficient embryos possess elevated apoptosis in the retina. Apoptotic cells are detected throughout the retina, surrounding the choroid fissure, and in the lens. (**C**) Quantitative analyses of *p53* levels show a 2.3-fold increase in *bcl6a*-SPMO injected embryos over *bcl6a*-MM controls. ($P < 0.0001$). (**D** and **E**) Embryos injected with 15 ng of *bcla*-MM develop normally. (**F** and **G**) Embryos injected with *bcl6a*-SPMO (7.5 ng) and *bcla*-MM (7.5 ng) present with colobomata (arrows). (**H** and **I**) Co-injection of *p53*-MO (7.5 ng) with *bcl6a*-SPMO (7.5 ng) suppresses colobomata (arrows).

$n = 3$ biological replicates, $P < 0.05$). Moreover, no enrichment was detected when a non-target region (~1 kb upstream) lacking a Vax2 binding sequence was probed in the anti-Myc ChIP sample (Fig. 5C).

As previously reported, *vax1* and *vax2*-MO injected embryos possessed colobomata (Fig. 5E–H). If Bcl6a mediates some of the downstream effects of Vax1 and Vax2 activity during eye development, we reasoned that Vax1 and Vax2 morpholino-injected embryos would also possess elevated apoptosis and *p53* levels. TUNEL analysis at 48 hpf showed apoptotic cells in the retinas of 68% of the *vax1* and *vax2*-MO injected embryos ($n = 19$), while no apoptotic cells were detected in the retinas of conMO injected embryos ($n = 21$) (Fig. 5I and J). qRT–PCR data revealed that *p53* expression in *vax1* and *2*-MO injected embryos was 4.4 times higher than that in conMO injected embryos ($P < 0.0001$) (Fig. 5D). To determine whether elevated *p53* levels in Vax1 and Vax2-deficient embryos contribute to increased apoptosis and colobomata, we determined whether these defects could be rescued by reducing p53 levels through morpholino knockdown, as was successful for Bcl6a morphants. Indeed, 86% of *vax1 and 2*-MO injected embryos co-injected with *p53*-MO developed normally, with no colobomata (Fig. 5K and L) and no detectable apoptotic cells ($n = 22$; Fig. 5M). These results support a model in which Vax1 and Vax2 function as upstream regulators of *bcl6a*, with Vax2 directly binding to the upstream regulatory elements of *bcl6a*, and that this regulatory network functions to repress *p53* expression and thereby block apoptosis in the developing optic cup.

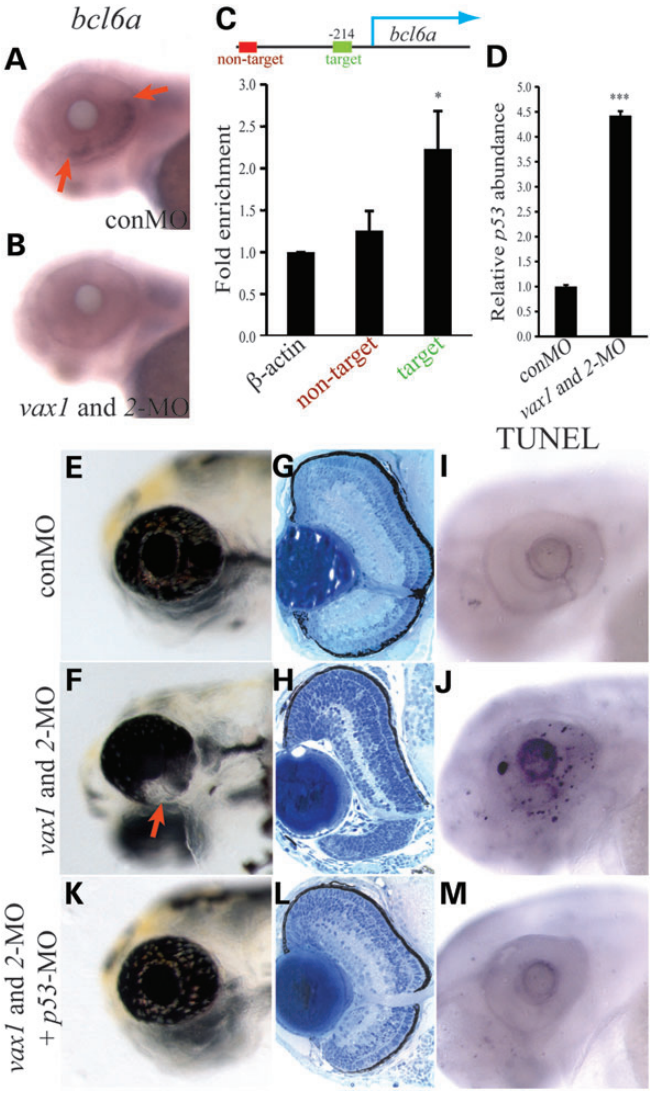

Figure 5. Vax1 and Vax2 function upstream of *bcl6a. bcl6a* expression in (**A**) conMO and (**B**) *vax1* and *vax2*-MO injected embryos at 48 hpf. (B) *bcl6* is not detected in *vax1* and *vax2*-MO injected embryos. (**C**) ChIP assays were performed with *myc-vax2* mRNA injected embryos, and enrichment of the Vax2 binding site containing region (Green) and a non-target region (Red) upstream of *bcl6a* was assessed by a qRT–PCR and normalized to β-actin expression. The Vax2 target region was enriched 2.23-fold in anti-Myc ChIP over that in the negative control ChIP ($n = 3$ biological replicates, $P < 0.05$), while the non-target region was not significantly enriched. (**E** and **F**) Loss of Vax1 and Vax2 results in colobomata (arrow). (**G** and **H**) Transverse histological section of *vax1* and *vax2*-MO injected embryos at 3 dpf shows obvious colobomata and extrusion of retinal and RPE tissue into the forebrain. TUNEL analysis in (**I**) conMO and (**J**) *vax1* and *vax2*-MO injected embryos at 48 hpf. Vax1 and Vax2-deficient embryos possess increased apoptosis in the retina. (**D**) *p53* levels are elevated 5.4-fold in *vax1* and *2*-MO injected embryos ($P < 0.0001$). (**K**–**M**) Co-injection of *p53*-MO reduces apoptotic cells and incidence of colobomata in *vax1* and *2*-MO injected embryos.

Bcor and Bcl6a functionally interact to prevent colobomata

Ng *et al*. reported colobomata in *bcor*-MO injected embryos (8), and we verified this observation at 3 dpf after injection of 1 ng of *bcor*-MO (Fig. 6A and B). The eyes from Bcor-deficient embryos showed severe colobomata, with many displaying medial displacement of the eye, as well as extruded retina/RPE tissue into the forebrain, making many appear as if they entirely lacked ventral retina (Fig. 6B and D). We hypothesized that Bcor deficiency would also lead to elevated *p53* levels and apoptosis, given its known functional interactions with Bcl6a in mediating Bcl6a-dependent transcriptional repression. TUNEL analysis at 48 hpf demonstrated elevated apoptosis in the retina of *bcor*-MO injected embryos, while no apoptotic cells were detected in the retina of conMO injected embryos (Fig. 6E and F). qRT–PCR revealed a 5.4-fold increase of *p53* expression in *bcor*-MO injected embryos over that in conMO injected embryos ($P < 0.0001$) (Fig. 6G). These results demonstrate that Bcor deficiency results in similar molecular phenotypes to Bcl6a deficiency, and suggest that Bcor may function *in vivo* as a cofactor for Bcl6a during normal eye development.

In vitro studies have demonstrated that Bcor co-immunoprecipitates with Bcl6 in B cells, suggesting that Bcor is found in a physical complex along with Bcl6 (15). We tested several polyclonal antibodies derived to Bcl6a and Bcor but could not find any that cross-reacted with the zebrafish proteins that would allow us to test this interaction biochemically. Thus, to determine whether Bcor functionally interacts with Bcl6a during eye development, we performed a synergistic interaction analysis. In these experiments, sub-threshold levels of different transcript-targeting morpholinos are injected to generate sensitized conditions, but no phenotypes. Then, embryos co-injected with both morpholinos at these sub-threshold levels are assayed for phenotypic defects; if defects are observed, a functional interaction between the two gene products *in vivo* is supported. To generate sensitized conditions, the amount of injected *bcl6a*-SPMO was reduced from 7.5 to 1.5 ng, and the amount of injected *bcor*-MO was reduced from 1 to 0.5 ng. These sub-threshold levels did not result in any observable phenotypes (Fig. 6H–M). Co-injection of these sub-threshold levels of *bcl6a*-SPMO and *bcor*-MO, however, resulted in colobomata in 68% of injected embryos ($n = 31$) (Fig. 6N and O). Thus, synergistic interaction data support a model in which Bcl6a and Bcor functionally interact during normal eye development to prevent colobomata.

Rnf2 and Bcor functionally interact to prevent colobomata

As discussed above, Rnf2 is a component of the Bcor repression complex (15). Rnf2 possesses E3 ubiquitin ligase activity and is thought to function as an effector protein of the Bcor complex wherein it helps to maintain chromatin in a transcriptionally repressed state by monoubiquitinating H2A. Interestingly, enriched monoubiquitinated H2A has been detected at the BCL6 target genes *Cyclin D2* and *p53* in B cells. *rnf2* is expressed in the zebrafish retina during development (68). Injection of 4 ng of an *rnf2*-MO targeting the 5′UTR of *rnf2* mRNA resulted in colobomata, as well as heart edema, and an absence of pectoral fins, defects previously reported in *rnf2* mutants and morphants (68) (Fig. 7A and B). Given the similarity in the phenotype to Bcl6a- and Bcor-deficient embryos, and its association with Bcor in the Bcor repression complex, we hypothesized that Rnf2 deficiency would also lead to elevated *p53* levels and apoptosis in the developing retina. Indeed, TUNEL analysis at 48 hpf demonstrated elevated apoptosis in the retinas of *rnf2*-MO injected embryos, while no apoptotic cells were detected in the retina of control embryos (Fig. 7C and D).

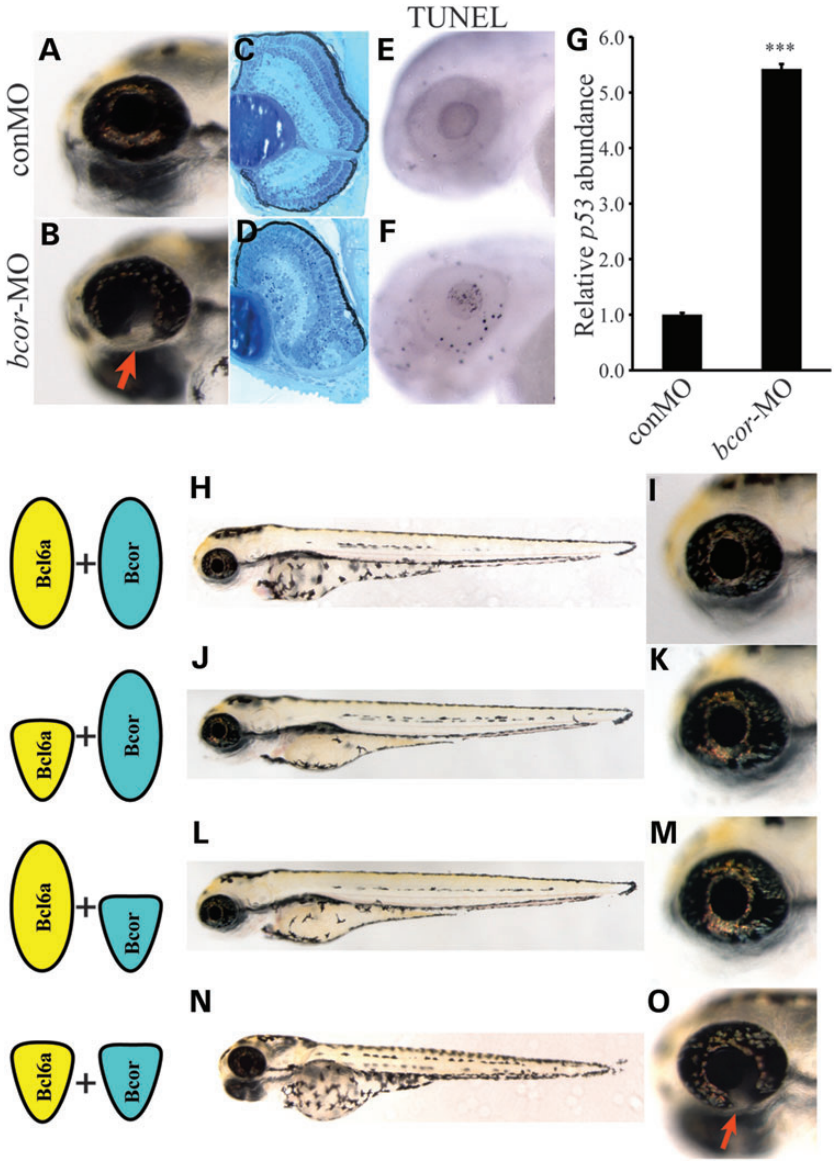

Figure 6. Knockdown of Bcor results in colobomata, increased apoptosis and elevated p53 levels, and Bcl6a and Bcor functionally interact in the eye. (**A** and **B**) Knockdown of Bcor results in colobomata (arrow in B). (**C** and **D**) In many *bcor*-MO injected embryos, the ventral retina is displaced medially. Transverse histological sectioning at 3 dpf highlights this displacement, appearing as if the ventral retina was absent. TUNEL analysis in (**E**) conMO and (**F**) *bcor*-MO injected embryos at 48 hpf. Bcor-deficient embryos present with an increased number of apoptotic cells in the retina. (**G**) Quantitative anaylsis by qRT–PCR shows a 5.4 fold increase of *p53* levels in *bcor*-MO injected embryos ($P < 0.0001$). (**H**–**O**) Synergistic interaction assays. (H and I) Embryos with wild-type levels of Bcl6 and Bcor develop normally. (J and K) Reducing the activity levels of Bcl6 by injecting sub-threshold amounts of *bcl6a*-SPMO (1.5 ng) has no effect on normal development. (L and M) Reducing the levels of Bcor by injecting sub-threshold amounts of *bcor*-MO (0.5 ng) has no effect on normal development. (N and O) Co-injection of sub-threshold amounts of *bcl6a*-SPMO (1.5 ng) and *bcor*-MO (0.5 ng) results in colobomata (arrow in O). Dorsal is up in all panels.

qRT–PCR revealed a 1.8-fold increase of *p53* expression in *rnf2*-MO injected embryos over that in conMO injected embryos ($P < 0.0001$) (Fig. 7E).

To determine whether Rnf2 functionally interacts with Bcor during eye development, we performed synergistic interaction analyses, as above. To generate sensitized conditions, the amount of injected *rnf2*-MO was reduced from 4 to 2 ng, and the amount of injected *bcor*-MO was reduced from 1 to 0.5 ng. These sub-threshold levels did not result in any observable phenotypes (Fig. 7F–K). Co-injection of these sub-threshold levels of *rnf2*-MO and *bcor*-MO, however, resulted in colobomata in 86% of injected embryos ($n = 22$) (Fig. 7L and M). These data support a model in which Rnf2 functions *in vivo* as an effector of the Bcl6a-recruited Bcor complex during normal eye development to prevent apoptosis and colobomatata.

Bcl6a and Bcor functionally interact with Hdacs to prevent colobomata

As discussed above, the transcriptional repressive function of Bcl6 requires Hdac activity in cell culture (69), and mutations in zebrafish *hdac1* result in colobomata (Fig. 8A and B)

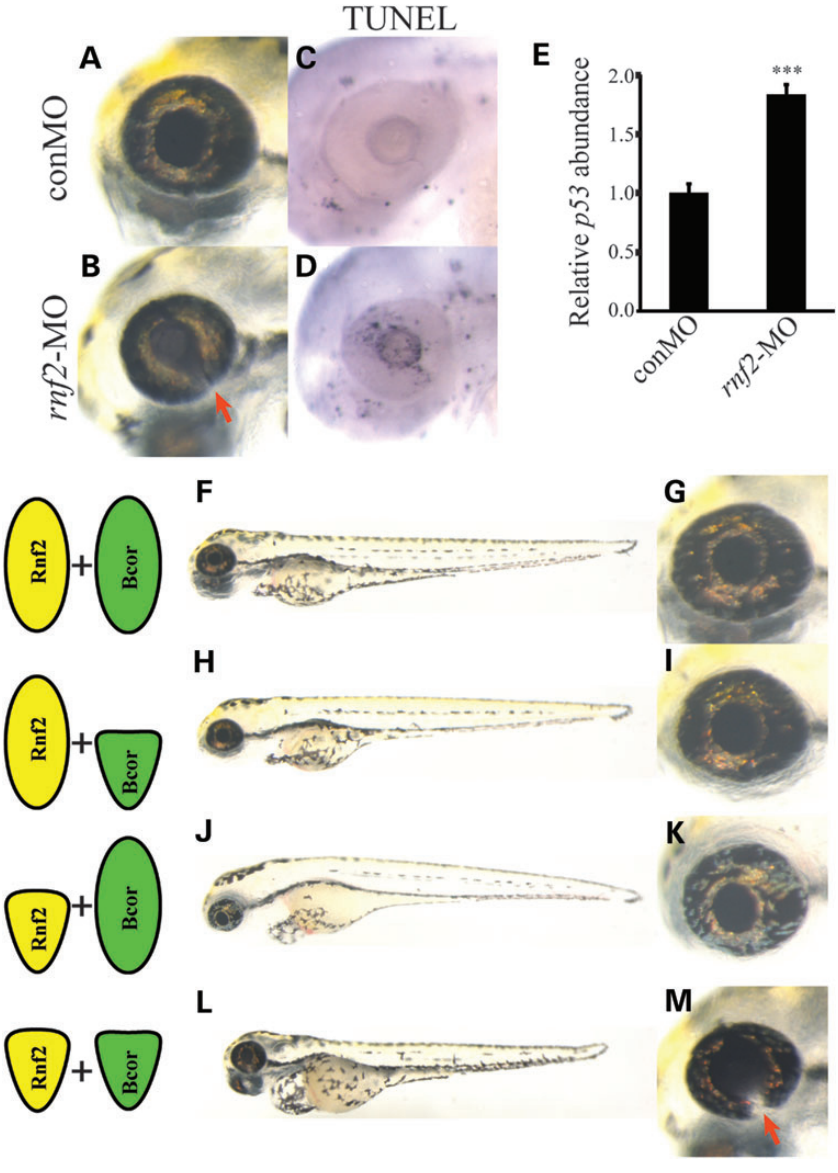

Figure 7. Knockdown of Rnf2 results in colobomata, increased apoptosis and elevated p53 levels, and Rnf2 and Bcor functionally interact in the eye. (**A** and **B**) Knockdown of Rnf2 results in colobomata (arrow in B). TUNEL analysis in (**C**) conMO and (**D**) *rnf2*-MO injected embryos at 48 hpf. Rnf2-deficient embryos present with an increased number of apoptotic cells in the retina. (**E**) Quantitative analysis by qRT–PCR shows a 1.8-fold increase of *p53* levels in *rnf2*-MO injected embryos ($P < 0.0001$). (**F** and **G**) Embryos with wild-type levels of Rnf2 and Bcor develop normally. (**H** and **I**) Reducing the levels of Bcor by injecting sub-threshold amounts of *bcor*-MO (0.5 ng) has no effect on normal development. (**J** and **K**) Reducing the activity levels of Rnf2 by injecting sub-threshold amounts of *rnf2*-MO (2 ng) has no effect on normal development. (**L** and **M**) Co-injection of sub-threshold amounts of *rnf2*-MO (2 ng) and *bcor*-MO (0.5 ng) results in colobomata (arrow in M). Dorsal is up in all panels.

(29,30). Moreover, Hdac1 is found associated with the Bcor repressive complex, along with Bcl6 (10). Thus, we hypothesized that Hdac function might also act as a mediator of Bcl6a and Bcor activity in the developing eye. To test this hypothesis, we first determined whether a mutation in *hdac1* results in elevated *p53* expression and apoptosis in the developing retina. Indeed, *p53* levels were significantly higher in *hdac1*$^{-/-}$ embryos than in wild-type controls at 48 hpf ($P < 0.0001$) (Fig. 8E), and *hdac1*$^{-/-}$ embryos possessed numerous apoptotic cells in their retinas (Fig. 8C and D). TSA is a chemical inhibitor of histone deacetylase activity, and previous studies have shown that TSA treatment (1200 nM, 14 hpf–48 hpf) phenocopies colobomata observed in *hdac1*$^{-/-}$ mutants (30). To determine whether functional interactions existed between Hdacs, Bcl6a and Bcor, we utilized subthreshold TSA exposures and performed synergistic interaction analyses, as above. Embryos treated with 700 nM TSA from 24 to 72 hpf (sub-threshold condition) developed normally and did not show colobomata (Fig. 8F–I; 9A–D). Embryos injected with 2 ng of *bcl6a*-SPMO also developed normally (Fig. 8J and K). However, treatment of 2 ng *bcl6a*-SPMO injected embryos with 700 nM TSA from 24 to 72 hpf resulted in embryos resembling *hdac1*$^{-/-}$ embryos, and their defects included obvious colobomata (81%, $n = 27$) (Fig. 8L and M). Similarly, embryos injected with sub-threshold

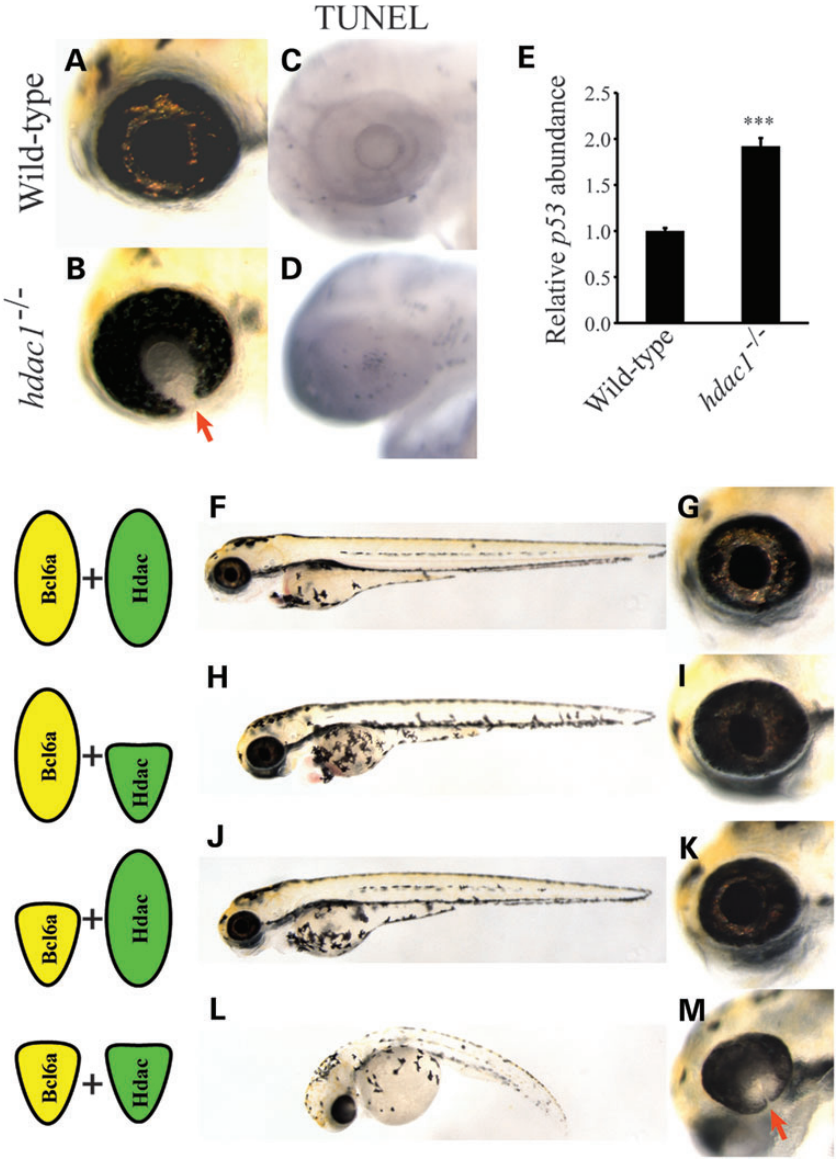

Figure 8. Bcl6a and Hdacs functionally interact in the eye. (**A** and **B**) *hdac1*$^{-/-}$ mutants embryos present with colobomata (arrow in B). TUNEL analysis in (**C**) wild-type and (**D**) *hdac1*$^{-/-}$ mutants embryos at 48 hpf. *hdac1*$^{-/-}$ mutants possess elevated apoptosis in the retina. (**E**) *p53* levels are elevated 1.9-fold in *hdac1*$^{-/-}$ mutants ($P < 0.0001$). (**F** and **G**) Embryos with wild-type levels of Bcl6a and Hdacs develop normally. (**H** and **I**) Reducing the activity levels of Hdacs by treating sub-threshold concentration of TSA (700 nM) has no effect on normal development. (**J** and **K**) Reducing the activity levels of Bcl6a by injecting sub-threshold amounts of *bcl6a*-SPMO (2 ng) has no effect on normal development. (**L** and **M**) Treatment of sub-threshold amounts of *bcl6a*-SPMO (2 ng) injected embryos with a sub-threshold concentration of TSA (700 nM) results in colobomata (arrow in M) and curved bodies. Dorsal is up in all panels.

amounts of *bcor*-MO (0.5 ng) developed normally (Fig. 9E and F). When 0.5 ng *bcor*-MO injected embryos were treated with 700 nM TSA from 24 to 72 hpf, they also possessed colobomata (86%, $n = 29$) (Fig. 9G and H). TSA is a broad-spectrum Hdac inhibitor so we next sought to determine whether Hdac1 specifically was required along with Bcor for normal eye development. To achieve this, we utilized *hdac1*$^{+/-}$ embryos as a sensitized condition, as these do not possess colobomata. Injection of sub-threshold *bcor*-MO into embryos from an *hdac1*$^{+/-}$ × WT cross resulted in 47.7% of the injected embryos ($n = 44$) possessing colobomata (Fig. 9I and J). Genotyping of five embryos with colobomata confirmed that all of them were genotypically *hdac1*$^{+/-}$. These data strongly support a model in which Hdac1 functionally interacts with Bcor during eye development and that, along with Bcl6a, act together to mediate normal optic cup formation by preventing colobomata.

DISCUSSION

A number of factors have been identified that lead to colobomata when mutated in human patients or from mutants, knockouts or loss-of-function experiments in a variety of animal model systems, but the molecular and cellular mechanisms underlying the colobomata in most of these cases have not been resolved (1,35). Here, we add another gene to the growing list of those

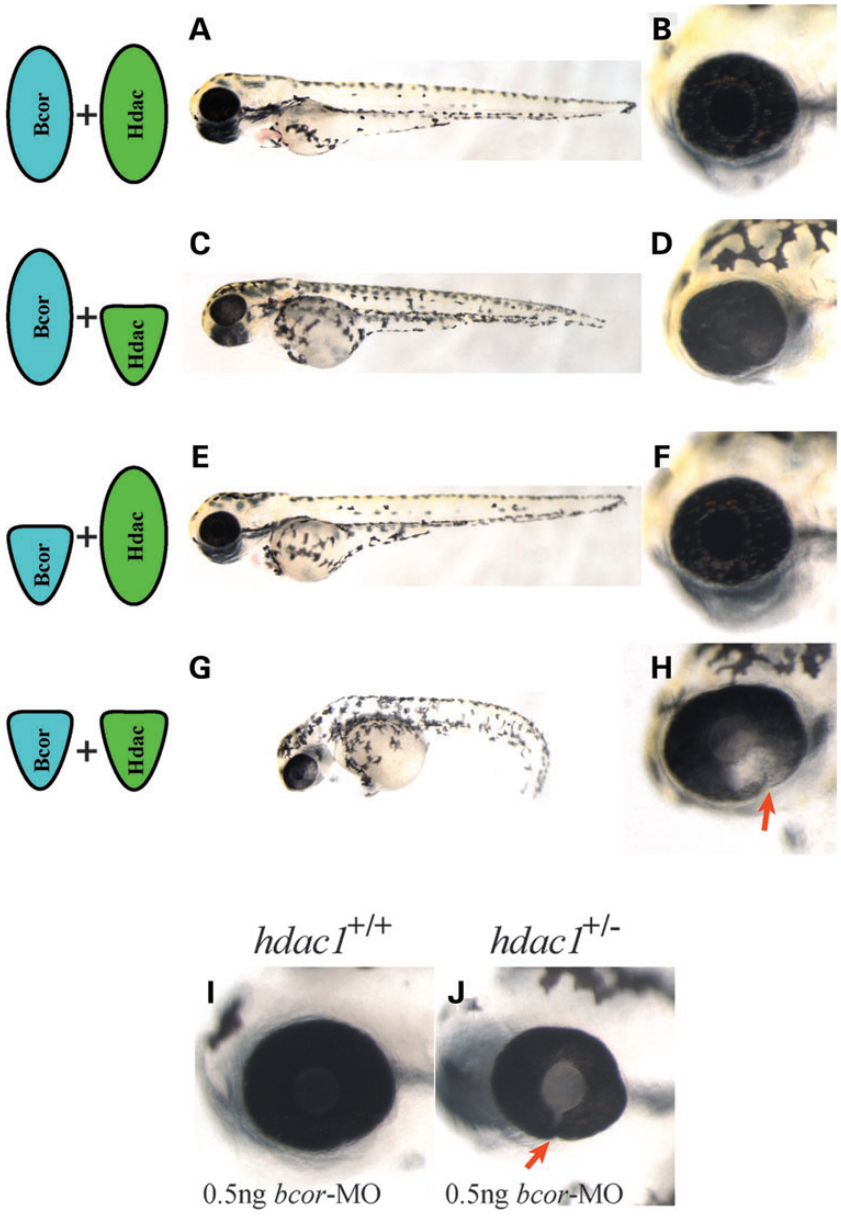

Figure 9. Bcor and Hdac1 functionally interact in the eye. (**A** and **B**) Embryos with wild-type levels of Bcor and Hdacs develop normally. (**C** and **D**) Reducing the activity levels of Hdacs by treating sub-threshold concentration of TSA (700 nM) has no effect on normal development. (**E** and **F**) Reducing the levels of Bcor by injecting sub-threshold amounts of *bcor*-MO (0.5 ng) has no effect on normal development. (**G** and **H**) Treatment of sub-threshold amounts of *bcor*-MO (0.5 ng) injected embryos with sub-threshold concentration of TSA (700 nM) results in colobomata (arrow in H) and curved bodies. (**I**) Injection of sub-threshold amounts of *bcor*-MO (0.5 ng) into wild-type siblings does not have any effect on normal development. (**J**) Injection of sub-threshold amounts of *bcor*-MO (0.5 ng) into *hdac1* $^{+/-}$ embryos results in colobomata.

required to prevent colobomata—*bcl6a*—and we demonstrate that it acts downstream of Vax1 and Vax2, well-known regulators of ventral optic cup development (40,52–55). Our data support a model in which *bcl6a* is a direct target of Vax2, where it functions to repress *p53* expression and prevent apoptosis in the developing optic cup. Furthermore, our data demonstrate that Bcl6a acts along with its co-repressor, Bcor, to prevent colobomata, and that both require Rnf2 and Hdac activity in order to achieve this (Fig. 10).

Bcl6 function is required in a variety of contexts to suppress apoptosis (23). Most notably is during immune system development when Bcl6 represses p53-dependent apoptosis that would otherwise result from DNA damage induced by immunoglobulin class switching and somatic hypermutation (22). Bcl6 has also been shown to repress the programmed cell death 2 gene (PDCD2) in lymphoma cell lines, and its expression is inverse to that of PDCD2 in lymphocytes and follicular mantle cells *in vivo* (70), suggestive of a critical role during immune system development and function. Bcl6 knockout mice display elevated levels of apoptosis during spermatogenesis (71), and Bcl6 is required for the survival of differentiating olfactory neurons (24). Indeed, in many cell types that express Bcl6,

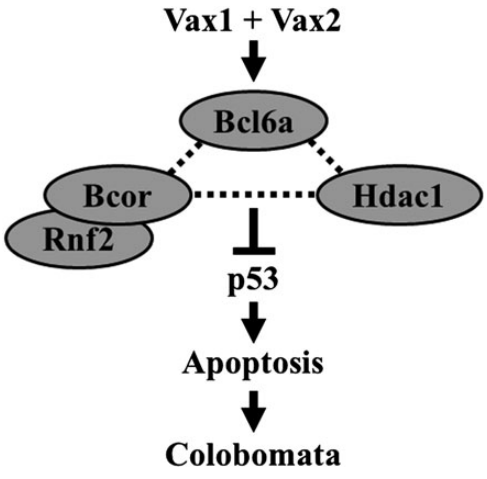

Figure 10. The Bcl6a-dependent regulatory network during zebrafish eye development. *bcl6a* expression requires Vax1 and Vax2 function, with Vax2 directly binding to the *bcl6a* upstream regulatory sequences. Bcl6a functions as a core factor in a gene regulatory network that includes Bcor, Rnf2 and Hdac in order to prevent apoptosis by repressing p53 expression during optic cup formation, thereby preventing colobomata.

terminal differentiation requires that apoptosis be inhibited, and it is thought that Bcl6 may mediate this inhibition (72–76). In various cell lines, sustained expression of Bcl6 confers a pro-survival effect, in some cases leading to oncogenic transformation (77). Importantly, however, sustained expression of Bcl6 is context-dependent as other cell lines and tissue types undergo apoptosis when Bcl6 levels are elevated (23).

During eye development in zebrafish, there are very few detectable apoptotic cells (63,78), indicating that either apoptosis is not critical for eye development or that it is suppressed in order for the eye to properly form. Data presented here support the latter of these hypotheses. Deletion of the cell death regulator *FADD* correlates with colobomata in human patients, and loss of *fadd* function in zebrafish leads to elevated cell death and colobomata (56). Cell death in Fadd-deficient embryos was shown to be necroptotic in nature, however. *fadd* expression is regulated by Pax2 and Vax2, supporting a gene regulatory network in which Pax2 and Vax2 act upstream of *fadd* to mediate cell survival in the developing optic cup. Our data place also Bcl6a in this cascade, downstream of Vax1 and Vax2, and they implicate Bcor, Rnf2 and Hdac as co-regulators required to suppress cell death in the eye. *p53* levels were elevated in embryos deficient for each of these factors, and inhibition of p53 expression rescued colobomata in all of them, supporting an underlying mechanism for colobomata prevention wherein Bcl6a and its co-repressors prevent *p53* expression and thus, prevent apoptotic cell death in the developing optic cup. Previous studies in zebrafish and mice lacking Vax1 and/or Vax2 function revealed that colobomata stemmed from a failure to restrict retinal cell fates to the optic cup (40,52–55). Our data, along with that of Viringipurampeer *et al*. for *fadd* (56), suggest an additional role for Vax1 and Vax2 during optic cup development in preventing apoptotic and necroptic cell death that would also lead to colobomata. Cell death is not restricted to the ventral optic cup in any of these perturbations, however. Moreover, while *bcl6a* expression is restricted to the ventral retina, *fadd*, *bcor, rnf2* and *hdac1* are expressed throughout the developing retina (68,79). Thus, cell death outside of the choroid fissure in loss-of-function embryos for each of these factors likely reflects additional pro-survival functions, possibly in combination with other DNA-recruitment factors, functioning similarly to Bcl6a, that are expressed in these retinal regions. Additionally, each of these proteins could function to repress the expression of other, cell non-autonomously acting factors that are pro-apoptotic in the retina.

Bcl6 is known to require co-factors in order to repress transcription of target genes, and these include BCOR and HDACs (10,69). Evidence from cultured cells demonstrates that Bcl6 interacts with Bcor through its POZ/BTB domain and recruits Bcor with other corepressors to Bcl6 target genes like *p53* and *cyclin D2* (15). Mutations in *BCOR* are responsible for OFCD syndrome (8), and loss of BCOR function results in colobomata in zebrafish and *Xenopus* embryos (8,11). Moreover, loss of either Bcl6 or Bcor function in *Xenopus* embryos also leads to laterality defects (11,25), and our data indicate conserved functions for Bcl6a; *Xenopus* embryos deficient in Bcl6 function possess colobomata (Fig. 3G and H), and zebrafish deficient in Bcl6a possess laterality defects (Supplementary Material, Fig. S2). Moreover, the synergistic interaction data reported here for Bcl6a and Bcor indicate that Bcl6a and Bcor functionally interact with each other *in vivo*, and this interaction is required for normal eye development.

HDACs are known to be involved in silencing transcription through the epigenetic modification of histones, maintaining a transcriptionally inactive chromatin state (80), or through directly regulating the activity of transcription activators by controlling their cytosolic/nuclear localization, affinities with co-factors or abilities to bind DNA (81). It has also been reported that acetylation of BCL6 by p300 inactivates its function as a transcriptional repressor and prevents it from recruiting HDACs to a repression complex (69). Zebrafish *hdac1* mutants possess severe colobomata and defects in cell cycle exit and differentiation of proliferative retinoblasts (29,30). In the developing mouse retina, HDAC activity is involved in regulating expression of the pro-apoptotic factors like Apaf-1 and Caspase3 in order to prevent apoptosis (31,32). Our interaction data between Bcl6a, Bcor and Hdac1 support a model in which these factors functionally interact with each other during eye development to repress *p53* expression to prevent apoptosis and colobomata.

Although Bcl6 function, target genes and corepressors have been studied in various contexts, the molecular mechanisms by which Bcl6 acts to suppress transcription remain to be elucidated. Bcl6 recruits the BCOR repression complex to target loci, and this complex also includes FBXL10 and RNF2 (15). RNF2 possesses E3 ubiquitin ligase activity for H2A, which facilitates the maintenance of repressed chromatin and thus, Bcl6-mediated recruitment of an RNF2-containing BCOR complex to target gene promoters could mediate transcriptional repression. Our data support a model in which Rnf2 functionally interacts with Bcor and is required to prevent colobomata. FBXL10, another BCOR complex member, demethylates H3K36 and could represent an additional biochemical mechanism through which Bcl6-mediated regulation leads to transcriptional repression. Interestingly, Fbxl10-deficient mice possess retinal colobomata and exencephaly correlating with increased cell death of neural progenitor cells (82). It will be of interest

to determine the molecular mechanisms through which Bcl6a acts in order to repress *p53* and prevent apoptosis and colobomata during optic cup formation, and to determine whether Bcl6a's functions are also mediated through the Bcor complex member, Fbxl10 in mediating this repression.

MATERIALS AND METHODS

Zebrafish maintenance and strains

Zebrafish (*Danio rerio*) were maintained at 28.5°C on a 14 h light/10 h dark cycle. Embryos were obtained from the natural spawning of wild-type (AB) fish setup in pairwise crosses. Embryos were collected and raised at 28.5°C after Westerfield (1995) and were staged according to Kimmel *et al*. (1995). *hdac1*^{hi1618Tg} outcrosses were provided by the Zebrafish International Resource Center at the University of Oregon and were propagated by repeated outcrosses to AB fish. All animals were treated in accordance with provisions established at the University of Texas at Austin governing animal use and care. *hdac1*^{hi1618Tg} mutants were genotyped by PCR (forward primer: 5′-CTG ACC TTG ATC TGA ACT TCT CTA TTC-3′) (reverse primer: 5′-CAC GCC TAC AGT GAT GGA ACC).

Histology

Histology was performed as described in Nuckels and Gross (2007). Briefly, embryos were collected and fixed overnight at 4°C in a solution of 1% (w/v) paraformaldehyde (PFA), 2.5% glutaraldehyde and 3% sucrose in phosphate buffered saline (PBS). They were washed three times for 5 min (min) in PBS, re-fixed for 90 min at 4°C in a 2% OsO_4 solution, washed three times for 5 min in PBS at room temperature (RT) and dehydrated through a graded ethanol series (50, 70, 80, 90, 2× 100%). Embryos were further dehydrated two times 10 min in propylene oxide and infiltrated 1–2 h in a 50% propylene oxide/50% Epon/Araldite mixture (Polysciences, Inc.). Embryos were then incubated overnight at RT in 100% Epon/Araldite resin with caps open to allow for propylene oxide evaporation and resin infiltration, embedded and baked at 60°C for 2–3 days. Sections 1–1.25 μm were cut, mounted on glass slides and stained in a 1% methylene blue/1% borax solution. Sections were mounted in DPX (Electron Microscopy Sciences) and photographed with a Leica DMRB microscope mounted with a DFC320 digital camera.

Morpholino and mRNA injections

bcl6a-SPMO (5′-GCA AGC AGC CTT CAA TTG TAC CTG C-3′), *bcl6a*-ATGMO (5′-TGT CGG CTG CAC AAG CCA TTT TTT C-3′), *bcl6a*-MM (5′-GGA AGC ACC CTT GAA TTC TAC GTG C-3′), *bcor*-MO (5′-AGC TCT CTT ACC GGA AAG AAA ACA C-3′) (8), *xbcl6*-MO (5′-TTG AGT TTG AGA TGC CAT AGT GCC C-3′), *p53*-MO (5′-GCG CCA TTG CTT TGC AAG AAT TG-3′) (83), *vax1*-MO (5′-GTC TTG ACT GTA GCG GAC TTC CAT A-3′) (40), *vax2*-MO (5′-ATG TGT CCA CTT AGT TTT CTT GAG C-3′) (40), *rnf2*-MO (5′-ACA CCA CGT CTT TTA TCT CAA TGT T-3′) (68) and conMO (5′-CCT CTT ACC TCA GTT ACA ATT TAT A-3′) were purchased from Gene Tools (Philomath, OR, USA). MOs were resuspended in water and injections were performed at the one-cell stage into wild-type Oregon AB embryos.

Full-length zebrafish *bcl6a* was sub-cloned from clone 4145622 (Open Biosystems) for mRNA synthesis (details available upon request). Capped mRNA synthesized using mMESSAGE mMACHINE (Ambion).

Riboprobes, *in situ* hybridization and immunohistochemistry

Hybridizations were performed essentially as described by Jowett and Lettice using digoxigenin-labeled antisense RNA probes (84). *p53* was cloned from 24 hpf complementary DNA (cDNA), ligated into pGEM-T and used for probe synthesis (cloning details available upon request). Probe synthesis constructs for *bcl6a* were purchased from Open Biosystems.

Immunohistochemistry with pH3 antiserum (Millipore) was performed as described by Uribe and Gross (2007). Imaging was performed on a Zeiss LSM5 Pascal laser scanning confocal microscope. Five to eight optical sections (1 μm in thickness) were collected and projected using Zeiss confocal software.

Trichostatin A (TSA) treatment

TSA stock solution (Sigma, 1 mg/ml in DMSO) was diluted in fish water for use. Embryos were incubated in TSA-containing fish water from 24 to 72 hpf and washed three times in fish water before imaging.

Preparation of *Xenopus* embryos and morpholino injection

Xenopus laevis embryos were de-jellied using a 3% cysteine solution in 1/3× MMR (Marc's Modified Ringers). *xbcl6*-MO was injected into one of dorsal cells at the four-cell stage and embryos were grown until stage 41 when they were fixed with 1× MEMFA (0.1 M MOPS, 2 mM EGTA, 1 mM $MgSO_4$, 3.7% formaldehyde, pH 7.4), and imaged on a Leica MZ16F microscope mounted with a DFC480 digital camera.

Quantitative real-time RT–PCR (qRT–PCR)

Total RNA was extracted from embryos at 48 hpf using TRIzol reagent (Invitrogen). The total RNA was reverse-transcribed using an iScript™ cDNA Synthesis kit (BIO-RAD). Relative gene expression levels were quantified using Power SYBR Green dye (Applied Biosystems) and an ABI PRISM 7900HT real-time PCR cycler (ABI SDS 2.3 software). All samples were analyzed in triplicate and relative transcript abundance was normalized to expression of *β-actin* using the 2 (-delta delta C(T)) method (85). Primers used to assay gene expression were designed across exon boundaries of the genes. Primers were as follows: *p53* forward 5′-CCC ATC CTC ACA ATC ATC ACT CTG G-3′, reverse 5′-TCT CCT CAG TTT TCC TGT CTC TGC C-3′; *β-actin* forward 5′- CCA AAG CCA ACA GAG AGA AGA TGA C-3′, reverse 5′- TAC AGA GAG AGC ACA GCC TGG ATG -3′. qRT–PCR data were analysed by Student's *t*-test for statistical significance.

Chromatin immunoprecipitation (ChIP) assay

ChIP assays were performed using a protocol modified by Wardle *et al*. (86). For exogenous Vax2 expression, embryos were injected with 170 pg of myc-tagged zebrafish *vax2* mRNA (subcloning details available upon request). Approximately 200 injected embryos were dechorionated and then cross-linked with 1.8% formaldehyde in fish water and incubated for 20 min at RT. Formaldehyde was deactivated by adding 2.5 M glycine (125 mM final concentration). Cross-linked embryos were homogenized in ChIP dilution buffer (0.1% SDS, 1% triton X-100, 2 m EDTA, 20 mm Tris-Cl pH 8.1, 150 mM NaCl, and protease inhibitors) with a 30G syringe and then sonicated using bioruptor (Diagenode) with conditions of: high power, 30 s on and 1 min off for 30 min. The lysate, containing an average size of 300–500 bp DNA fragments, was precleared with protein A agarose beads at 4°C for 3 h to minimize non-specific binding. Precleared chromatin was incubated with an anti-Myc tag antibody (ab9106, Abcam) or an anti-fibronectin antibody (sc-9068, Santa Cruz Biotechnology) (as a negative control) at 4°C overnight. Protein–DNA complexes were pulled down using prewashed protein A agarose beads at 4°C for 6 h. Immunoprecipitated complexes were washed twice for 5 min with a low salt wash buffer (1% Triton X-100, 1 mM EDTA, 50 mM HEPES pH 7.5, 0.1% sodium deoxycholate, 150 mM NaCl), once with a high-salt wash buffer (1% Triton X-100, 1 mM EDTA, 50 mM HEPES pH 7.5, 0.1% sodium deoxycholate, 500 mM NaCl), once with a LiCl wash buffer (250 mM LiCl, 0.5% NP-40, 1 mM EDTA, 0.5% sodium deoxycholate, 10 mM Tris–Cl pH 8.1), and twice with TE buffer (10 mM Tris-Cl pH 7.5, 1 mM EDTA). SDS elution buffer was applied to the washed sample to recover protein–DNA complexes at 65°C for 30 min. Immunoprecipitated DNA was further decross-linked by incubating at 65°C overnight in SDS elution buffer. RNA and Proteins were removed by treating with RNase A and Proteinase K followed by phenol–chloroform extraction and ethanol precipitation The DNA pellet from ethanol precipitation was resuspended in 20 μl of TE buffer. Three separate ChIP experiments were performed with three separate batches of injected embryos (i.e. three biological replicates). Enriched DNA was utilized for qRT–PCRs. Primers were as follows: Target forward 5′-CGT GTT TTG CTT TAA GTT TGC ATT TCT TCG G-3′, reverse 5′-GTG CCA CTA TTT TTC TCA ATC GTT ACG GC-3′; negative control forward 5′-CCC TCA CGT TGA AAC TCG ATG ACA G-3′, reverse 5′-CAA AGA CCG TTC ACG AGC AAA CAG-3′. Relative abundance was normalized to expression of *β-actin* and compared between ChIPs using anti-Myc and ant-Fibronectin antibodies. qRT–PCR data were analyzed by Student's *t*-test for statistical significance.

Terminal deoxynucleotidyl transferase dUTP nick end labeling (TUNEL) analysis

Apoptotic cells were examined by TUNEL. Embryos were fixed overnight in 4% paraformaldehyde at 4°C, washed three times with PBS and dehydrated in 100% methanol at −20°C. Rehydration of the embryos through a degraded methanol/PBS series (50, 30, 0%) for 5 min each at RT was followed by incubation in 100% acetone at −20°C (12 min) and three washes in PBS containing 0.1% Tween-20 (PBST) for 5 min each. The embryos were permeabilized with 10 μg/ml proteinase K for 25 min at RT, followed by 4% paraformaldehyde and three rinses in PBST. The embryos were assayed by TUNEL using the *In Situ* Cell Death Detection kit, AP (Roche), and the images were examined by light microscopy on a Leica MZ16F microscope mounted with a DFC480 digital camera.

SUPPLEMENTARY MATERIAL

Supplementary Material is available at *HMG* online.

ACKNOWLEDGEMENTS

We are grateful to John Wallingford and his laboratory for assistance with *Xenopus* experiments, to John Reis for technical assistance and to members of the Gross laboratory for advice and criticism throughout this project.

FUNDING

This work was supported by grants from the National Science Foundation (CAREER Award IOS-0745782) and National Institutes of Health (RO1-EY18005). Zebrafish were obtained from ZIRC, which is supported by NIH-NCRR Grant P40 RR012546.

REFERENCES

1. Chang, L., Blain, D., Bertuzzi, S. and Brooks, B.P. (2006) Uveal coloboma: clinical and basic science update. *Curr. Opin. Ophthalmol.*, **17**, 447–470.
2. Fitzpatrick, D.R. and van Heyningen, V. (2005) Developmental eye disorders. *Curr. Opin. Genet. Dev.*, **15**, 348–353.
3. Gregory-Evans, C.Y., Williams, M.J., Halford, S. and Gregory-Evans, K. (2004) Ocular coloboma: a reassessment in the age of molecular neuroscience. *J. Med. Genet.*, **41**, 881–891.
4. Hornby, S.J., Gilbert, C.E., Rahi, J.K., Sil, A.K., Xiao, Y., Dandona, L. and Foster, A. (2000) Regional variation in blindness in children due to microphthalmos, anophthalmos and coloboma. *Ophthalmic Epidemiol.*, **7**, 127–138.
5. Porges, Y. (1995) Autosomal dominant typical coloboma associated with unilateral pseudoptosis, myopia and cataract. *Cent Afr. J. Med.*, **41**, 255–257.
6. Gorlin, R.J., Marashi, A.H. and Obwegeser, H.L. (1996) Oculo-facio-cardio-dental (OFCD) syndrome. *Am. J. Med. Genet.*, **63**, 290–292.
7. Hedera, P. and Gorski, J.L. (2003) Oculo-facio-cardio-dental syndrome: skewed X chromosome inactivation in mother and daughter suggest X-linked dominant inheritance. *Am. J. Med. Genet. A*, **123A**, 261–266.
8. Ng, D., Thakker, N., Corcoran, C.M., Donnai, D., Perveen, R., Schneider, A., Hadley, D.W., Tifft, C., Zhang, L., Wilkie, A.O. *et al.* (2004) Oculofaciocardiodental and Lenz microphthalmia syndromes result from distinct classes of mutations in BCOR. *Nat. Genet.*, **36**, 411–416.
9. Schulze, B.R., Horn, D., Kobelt, A., Tariverdian, G. and Stellzig, A. (1999) Rare dental abnormalities seen in oculo-facio-cardio-dental (OFCD) syndrome: three new cases and review of nine patients. *Am. J. Med. Genet.*, **82**, 429–435.
10. Huynh, K.D., Fischle, W., Verdin, E. and Bardwell, V.J. (2000) BCoR, a novel corepressor involved in BCL-6 repression. *Genes Dev.*, **14**, 1810–1823.
11. Hilton, E.N., Manson, F.D., Urquhart, J.E., Johnston, J.J., Slavotinek, A.M., Hedera, P., Stattin, E.L., Nordgren, A., Biesecker, L.G. and Black, G.C. (2007) Left-sided embryonic expression of the BCL-6 corepressor, BCOR, is required for vertebrate laterality determination. *Hum. Mol. Genet.*, **16**, 1773–1782.

12. Tsukada, Y., Fang, J., Erdjument-Bromage, H., Warren, M.E., Borchers, C.H., Tempst, P. and Zhang, Y. (2006) Histone demethylation by a family of JmjC domain-containing proteins. *Nature*, **439**, 811–816.
13. Bannister, A.J., Schneider, R., Myers, F.A., Thorne, A.W., Crane-Robinson, C. and Kouzarides, T. (2005) Spatial distribution of di- and trimethyl lysine 36 of histone H3 at active genes. *J. Biol. Chem.*, **280**, 17732–17736.
14. Rao, B., Shibata, Y., Strahl, B.D. and Lieb, J.D. (2005) Dimethylation of histone H3 at lysine 36 demarcates regulatory and nonregulatory chromatin genome-wide. *Mol. Cell Biol.*, **25**, 9447–9459.
15. Gearhart, M.D., Corcoran, C.M., Wamstad, J.A. and Bardwell, V.J. (2006) Polycomb group and SCF ubiquitin ligases are found in a novel BCOR complex that is recruited to BCL6 targets. *Mol. Cell Biol.*, **26**, 6880–6889.
16. Chang, C.C., Ye, B.H., Chaganti, R.S. and Dalla-Favera, R. (1996) BCL-6, a POZ/zinc-finger protein, is a sequence-specific transcriptional repressor. *Proc. Natl Acad. Sci. USA*, **93**, 6947–6952.
17. Seyfert, V.L., Allman, D., He, Y. and Staudt, L.M. (1996) Transcriptional repression by the proto-oncogene BCL-6. *Oncogene*, **12**, 2331–2342.
18. Baron, B.W., Nucifora, G., McCabe, N., Espinosa, R. 3rd, Le Beau, M.M. and McKeithan, T.W. (1993) Identification of the gene associated with the recurring chromosomal translocations t(3;14)(q27;q32) and t(3;22)(q27;q11) in B-cell lymphomas. *Proc. Natl Acad. Sci. USA*, **90**, 5262–5266.
19. Kerckaert, J.P., Deweindt, C., Tilly, H., Quief, S., Lecocq, G. and Bastard, C. (1993) LAZ3, a novel zinc-finger encoding gene, is disrupted by recurring chromosome 3q27 translocations in human lymphomas. *Nat. Genet.*, **5**, 66–70.
20. Ye, B.H., Rao, P.H., Chaganti, R.S. and Dalla-Favera, R. (1993) Cloning of bcl-6, the locus involved in chromosome translocations affecting band 3q27 in B-cell lymphoma. *Cancer Res.*, **53**, 2732–2735.
21. Dent, A.L., Shaffer, A.L., Yu, X., Allman, D. and Staudt, L.M. (1997) Control of inflammation, cytokine expression, and germinal center formation by BCL-6. *Science*, **276**, 589–592.
22. Phan, R.T. and Dalla-Favera, R. (2004) The BCL6 proto-oncogene suppresses p53 expression in germinal-centre B cells. *Nature*, **432**, 635–639.
23. Albagli-Curiel, O. (2003) Ambivalent role of BCL6 in cell survival and transformation. *Oncogene*, **22**, 507–516.
24. Otaki, J.M., Hatano, M., Matayoshi, R., Tokuhisa, T. and Yamamoto, H. The proto-oncogene BCL6 promotes survival of olfactory sensory neurons. *Dev. Neurobiol.*, **70**, 424–435.
25. Sakano, D., Kato, A., Parikh, N., McKnight, K., Terry, D., Stefanovic, B. and Kato, Y. BCL6 canalizes Notch-dependent transcription, excluding Mastermind-like1 from selected target genes during left-right patterning. *Dev. Cell*, **18**, 450–462.
26. Dhordain, P., Albagli, O., Lin, R.J., Ansieau, S., Quief, S., Leutz, A., Kerckaert, J.P., Evans, R.M. and Leprince, D. (1997) Corepressor SMRT binds the BTB/POZ repressing domain of the LAZ3/BCL6 oncoprotein. *Proc. Natl Acad. Sci. USA*, **94**, 10762–10767.
27. Dhordain, P., Lin, R.J., Quief, S., Lantoine, D., Kerckaert, J.P., Evans, R.M. and Albagli, O. (1998) The LAZ3(BCL-6) oncoprotein recruits a SMRT/mSIN3A/histone deacetylase containing complex to mediate transcriptional repression. *Nucleic Acids Res.*, **26**, 4645–4651.
28. Wong, C.W. and Privalsky, M.L. (1998) Components of the SMRT corepressor complex exhibit distinctive interactions with the POZ domain oncoproteins PLZF, PLZF-RARalpha, and BCL-6. *J. Biol. Chem.*, **273**, 27695–27702.
29. Stadler, J.A., Shkumatava, A., Norton, W.H., Rau, M.J., Geisler, R., Fischer, S. and Neumann, C.J. (2005) Histone deacetylase 1 is required for cell cycle exit and differentiation in the zebrafish retina. *Dev. Dyn.*, **233**, 883–889.
30. Yamaguchi, M., Tonou-Fujimori, N., Komori, A., Maeda, R., Nojima, Y., Li, H., Okamoto, H. and Masai, I. (2005) Histone deacetylase 1 regulates retinal neurogenesis in zebrafish by suppressing Wnt and Notch signaling pathways. *Development*, **132**, 3027–3043.
31. Wallace, D.M. and Cotter, T.G. (2009) Histone deacetylase activity in conjunction with E2F-1 and p53 regulates Apaf-1 expression in 661W cells and the retina. *J. Neurosci. Res.*, **87**, 887–905.
32. Wallace, D.M., Donovan, M. and Cotter, T.G. (2006) Histone deacetylase activity regulates apaf-1 and caspase 3 expression in the developing mouse retina. *Invest Ophthalmol. Vis. Sci.*, **47**, 2765–2772.
33. Gross, J.M. and Perkins, B.D. (2008) Zebrafish mutants as models for congenital ocular disorders in humans. *Mol. Reprod. Dev.*, **75**, 547–555.
34. Goldsmith, P. and Harris, W.A. (2003) The zebrafish as a tool for understanding the biology of visual disorders. *Semin Cell Dev. Biol.*, **14**, 11–18.
35. Bibliowicz, J., Tittle, R.K. and Gross, J.M. Toward a better understanding of human eye disease insights from the zebrafish, Danio rerio. *Prog. Mol. Biol. Transl. Sci.*, **100**, 287–330.
36. Erdmann, B., Kirsch, F.P., Rathjen, F.G. and More, M.I. (2003) N-cadherin is essential for retinal lamination in the zebrafish. *Dev. Dyn.*, **226**, 570–577.
37. Heisenberg, C.P., Brennan, C. and Wilson, S.W. (1999) Zebrafish aussicht mutant embryos exhibit widespread overexpression of ace (fgf8) and coincident defects in CNS development. *Development*, **126**, 2129–2140.
38. Macdonald, R., Scholes, J., Strahle, U., Brennan, C., Holder, N., Brand, M. and Wilson, S.W. (1997) The Pax protein Noi is required for commissural axon pathway formation in the rostral forebrain. *Development*, **124**, 2397–2408.
39. Torres, M., Gomez-Pardo, E. and Gruss, P. (1996) Pax2 contributes to inner ear patterning and optic nerve trajectory. *Development*, **122**, 3381–3391.
40. Take-uchi, M., Clarke, J.D. and Wilson, S.W. (2003) Hedgehog signalling maintains the optic stalk-retinal interface through the regulation of Vax gene activity. *Development*, **130**, 955–968.
41. Nakayama, Y., Miyake, A., Nakagawa, Y., Mido, T., Yoshikawa, M., Konishi, M. and Itoh, N. (2008) Fgf19 is required for zebrafish lens and retina development. *Dev. Biol.*, **313**, 752–766.
42. Masai, I., Lele, Z., Yamaguchi, M., Komori, A., Nakata, A., Nishiwaki, Y., Wada, H., Tanaka, H., Nojima, Y., Hammerschmidt, M. *et al.* (2003) N-cadherin mediates retinal lamination, maintenance of forebrain compartments and patterning of retinal neurites. *Development*, **130**, 2479–2494.
43. Malicki, J., Jo, H. and Pujic, Z. (2003) Zebrafish N-cadherin, encoded by the glass onion locus, plays an essential role in retinal patterning. *Dev. Biol.*, **259**, 95–108.
44. Nadauld, L.D., Chidester, S., Shelton, D.N., Rai, K., Broadbent, T., Sandoval, I.T., Peterson, P.W., Manos, E.J., Ireland, C.M., Yost, H.J. *et al.* (2006) Dual roles for adenomatous polyposis coli in regulating retinoic acid biosynthesis and Wnt during ocular development. *Proc. Natl Acad. Sci. USA*, **103**, 13409–13414.
45. Lee, J. and Gross, J.M. (2007) Laminin beta1 and gamma1 containing laminins are essential for basement membrane integrity in the zebrafish eye. *Invest. Ophthalmol. Vis. Sci.*, **48**, 2483–2490.
46. Lee, J., Willer, J.R., Willer, G.B., Smith, K., Gregg, R.G. and Gross, J.M. (2008) Zebrafish blowout provides genetic evidence for Patched1-mediated negative regulation of Hedgehog signaling within the proximal optic vesicle of the vertebrate eye. *Dev. Biol.*, **319**, 10–22.
47. Brown, J.D., Dutta, S., Bharti, K., Bonner, R.F., Munson, P.J., Dawid, I.B., Akhtar, A.L., Onojafe, I.F., Alur, R.P., Gross, J.M. *et al.* (2009) Expression profiling during ocular development identifies 2 Nlz genes with a critical role in optic fissure closure. *Proc. Natl Acad. Sci. USA*, **106**, 1462–1467.
48. Gestri, G., Osborne, R.J., Wyatt, A.W., Gerrelli, D., Gribble, S., Stewart, H., Fryer, A., Bunyan, D.J., Prescott, K., Collin, J.R. *et al.* (2009) Reduced TFAP2A function causes variable optic fissure closure and retinal defects and sensitizes eye development to mutations in other morphogenetic regulators. *Hum. Genet.*, **126**, 791–803.
49. Barbieri, A.M., Lupo, G., Bulfone, A., Andreazzoli, M., Mariani, M., Fougerousse, F., Consalez, G.G., Borsani, G., Beckmann, J.S., Barsacchi, G. *et al.* (1999) A homeobox gene, vax2, controls the patterning of the eye dorsoventral axis. *Proc. Natl Acad. Sci. USA*, **96**, 10729–10734.
50. Hallonet, M., Hollemann, T., Wehr, R., Jenkins, N.A., Copeland, N.G., Pieler, T. and Gruss, P. (1998) Vax1 is a novel homeobox-containing gene expressed in the developing anterior ventral forebrain. *Development*, **125**, 2599–2610.
51. Ohsaki, K., Morimitsu, T., Ishida, Y., Kominami, R. and Takahashi, N. (1999) Expression of the Vax family homeobox genes suggests multiple roles in eye development. *Genes Cells*, **4**, 267–276.
52. Barbieri, A.M., Broccoli, V., Bovolenta, P., Alfano, G., Marchitiello, A., Mocchetti, C., Crippa, L., Bulfone, A., Marigo, V., Ballabio, A. *et al.* (2002) Vax2 inactivation in mouse determines alteration of the eye dorsal–ventral axis, misrouting of the optic fibres and eye coloboma. *Development*, **129**, 805–813.
53. Bertuzzi, S., Hindges, R., Mui, S.H., O'Leary, D.D. and Lemke, G. (1999) The homeodomain protein vax1 is required for axon guidance and major tract formation in the developing forebrain. *Genes Dev.*, **13**, 3092–3105.

54. Hallonet, M., Hollemann, T., Pieler, T. and Gruss, P. (1999) Vax1, a novel homeobox-containing gene, directs development of the basal forebrain and visual system. *Genes Dev.*, **13**, 3106–3114.
55. Mui, S.H., Hindges, R., O'Leary, D.D., Lemke, G. and Bertuzzi, S. (2002) The homeodomain protein Vax2 patterns the dorsoventral and nasotemporal axes of the eye. *Development*, **129**, 797–804.
56. Viringipurampeer, I.A., Ferreira, T., Demaria, S., Yoon, J.J., Shan, X., Moosajee, M., Gregory-Evans, K., Ngai, J. and Gregory-Evans, C.Y. Pax2 regulates a fadd-dependent molecular switch that drives tissue fusion during eye development. *Hum. Mol. Genet.*, **21**, 2357–2369.
57. Gregory-Evans, C.Y., Moosajee, M., Hodges, M.D., Mackay, D.S., Game, L., Vargesson, N., Bloch-Zupan, A., Ruschendorf, F., Santos-Pinto, L., Wackens, G. *et al.* (2007) SNP genome scanning localizes oto-dental syndrome to chromosome 11q13 and microdeletions at this locus implicate FGF3 in dental and inner-ear disease and FADD in ocular coloboma. *Hum. Mol. Genet.*, **16**, 2482–2493.
58. Thisse, B., Heyer, V., Lux, A., Alunni, V., Degrave, A., Seiliez, I., Kirchner, J., Parkhill, J.P. and Thisse, C. (2004) Spatial and temporal expression of the zebrafish genome by large-scale *in situ* hybridization screening. *Methods Cell Biol.*, **77**, 505–519.
59. Nasevicius, A. and Ekker, S.C. (2000) Effective targeted gene 'knockdown' in zebrafish. *Nat. Genet.*, **26**, 216–220.
60. Draper, B.W., Morcos, P.A. and Kimmel, C.B. (2001) Inhibition of zebrafish fgf8 pre-mRNA splicing with morpholino oligos: a quantifiable method for gene knockdown. *Genesis*, **30**, 154–156.
61. Robu, M.E., Larson, J.D., Nasevicius, A., Beiraghi, S., Brenner, C., Farber, S.A. and Ekker, S.C. (2007) p53 activation by knockdown technologies. *PLoS Genet.*, **3**, e78.
62. Dale, L. and Slack, J.M. (1987) Fate map for the 32-cell stage of Xenopus laevis. *Development*, **99**, 527–551.
63. Cole, L.K. and Ross, L.S. (2001) Apoptosis in the developing zebrafish embryo. *Dev. Biol.*, **240**, 123–142.
64. Kim, T.H., Goodman, J., Anderson, K.V. and Niswander, L. (2007) Phactr4 regulates neural tube and optic fissure closure by controlling PP1-, Rb-, and E2F1-regulated cell-cycle progression. *Dev. Cell*, **13**, 87–102.
65. Blythe, S.A., Reid, C.D., Kessler, D.S. and Klein, P.S. (2009) Chromatin immunoprecipitation in early Xenopus laevis embryos. *Dev. Dyn*, **238**, 1422–1432.
66. Havis, E., Anselme, I. and Schneider-Maunoury, S. (2006) Whole embryo chromatin immunoprecipitation protocol for the *in vivo* study of zebrafish development. *Biotechniques*, **40**, 34–40.
67. Li, H., Lu, Y., Smith, H.K. and Richardson, W.D. (2007) Olig1 and Sox10 interact synergistically to drive myelin basic protein transcription in oligodendrocytes. *J. Neurosci.*, **27**, 14375–14382.
68. van der Velden, Y.U., Wang, L., van Lohuizen, M. and Haramis, A.P. The Polycomb group protein Ring1b is essential for pectoral fin development. *Development*, **139**, 2210–2220.
69. Bereshchenko, O.R., Gu, W. and Dalla-Favera, R. (2002) Acetylation inactivates the transcriptional repressor BCL6. *Nat. Genet.*, **32**, 606–613.
70. Baron, B.W., Anastasi, J., Thirman, M.J., Furukawa, Y., Fears, S., Kim, D.C., Simone, F., Birkenbach, M., Montag, A., Sadhu, A. *et al.* (2002) The human programmed cell death-2 (PDCD2) gene is a target of BCL6 repression: implications for a role of BCL6 in the down-regulation of apoptosis. *Proc. Natl Acad. Sci. USA*, **99**, 2860–2865.
71. Kojima, S., Hatano, M., Okada, S., Fukuda, T., Toyama, Y., Yuasa, S., Ito, H. and Tokuhisa, T. (2001) Testicular germ cell apoptosis in Bcl6-deficient mice. *Development*, **128**, 57–65.
72. Bajalica-Lagercrantz, S., Piehl, F., Farnebo, F., Larsson, C. and Lagercrantz, J. (1998) Expression of the BCL6 gene in the pre- and postnatal mouse. *Biochem. Biophys. Res. Commun.*, **247**, 357–360.
73. Funatsu, N., Inoue, T. and Nakamura, S. (2004) Gene expression analysis of the late embryonic mouse cerebral cortex using DNA microarray: identification of several region- and layer-specific genes. *Cereb. Cortex*, **14**, 1031–1044.
74. Logarajah, S., Hunter, P., Kraman, M., Steele, D., Lakhani, S., Bobrow, L., Venkitaraman, A. and Wagner, S. (2003) BCL-6 is expressed in breast cancer and prevents mammary epithelial differentiation. *Oncogene*, **22**, 5572–5578.
75. Otaki, J.M., Fearon, D.T. and Yamamoto, H. (2005) The proto-oncogene BCL-6 is expressed in olfactory sensory neurons. *Neurosci. Res.*, **53**, 189–200.
76. Leamey, C.A., Glendining, K.A., Kreiman, G., Kang, N.D., Wang, K.H., Fassler, R., Sawatari, A., Tonegawa, S. and Sur, M. (2008) Differential gene expression between sensory neocortical areas: potential roles for Ten_m3 and Bcl6 in patterning visual and somatosensory pathways. *Cereb. Cortex*, **18**, 53–66.
77. Shvarts, A., Brummelkamp, T.R., Scheeren, F., Koh, E., Daley, G.Q., Spits, H. and Bernards, R. (2002) A senescence rescue screen identifies BCL6 as an inhibitor of anti-proliferative p19(ARF)-p53 signaling. *Genes Dev.*, **16**, 681–686.
78. Biehlmaier, O., Neuhauss, S.C. and Kohler, K. (2001) Onset and time course of apoptosis in the developing zebrafish retina. *Cell Tissue Res.*, **306**, 199–207.
79. Thisse, C. and Thisse, B. (2008) High-resolution *in situ* hybridization to whole-mount zebrafish embryos. *Nat. Protoc.*, **3**, 59–69.
80. Sterner, D.E. and Berger, S.L. (2000) Acetylation of histones and transcription-related factors. *Microbiol. Mol. Biol. Rev.*, **64**, 435–459.
81. Barlev, N.A., Liu, L., Chehab, N.H., Mansfield, K., Harris, K.G., Halazonetis, T.D. and Berger, S.L. (2001) Acetylation of p53 activates transcription through recruitment of coactivators/histone acetyltransferases. *Mol. Cell*, **8**, 1243–1254.
82. Fukuda, T., Tokunaga, A., Sakamoto, R. and Yoshida, N. Fbxl10/Kdm2b deficiency accelerates neural progenitor cell death and leads to exencephaly. *Mol. Cell Neurosci.*, **46**, 614–624.
83. Langheinrich, U., Hennen, E., Stott, G. and Vacun, G. (2002) Zebrafish as a model organism for the identification and characterization of drugs and genes affecting p53 signaling. *Curr. Biol.*, **12**, 2023–2028.
84. Jowett, T. and Lettice, L. (1994) Whole-mount *in situ* hybridizations on zebrafish embryos using a mixture of digoxigenin- and fluorescein-labelled probes. *Trends Genet.*, **10**, 73–74.
85. Livak, K.J. and Schmittgen, T.D. (2001) Analysis of relative gene expression data using real-time quantitative PCR and the 2(-Delta Delta C(T)) Method. *Methods*, **25**, 402–408.
86. Wardle, F.C., Odom, D.T., Bell, G.W., Yuan, B., Danford, T.W., Wiellette, E.L., Herbolsheimer, E., Sive, H.L., Young, R.A. and Smith, J.C. (2006) Zebrafish promoter microarrays identify actively transcribed embryonic genes. *Genome Biol.*, **7**, R71.